PROCEEDINGS OF SCIENCE

# FAST NEUTRON SCATTERING ON CARBON AND OXYGEN

**P. Mermod**[*], **J. Blomgren**[†], **M. Hayashi, L. Nilsson, S. Pomp, A. Öhrn, M. Österlund**

*Department of Neutron Research, Uppsala University, Box 525, S-75120 Uppsala, Sweden*

**A. Prokofiev**

*The Svedberg Laboratory, Uppsala University, Uppsala, Sweden*

**U. Tippawan**

*Fast Neutron Research Facility, Chiang Mai University, Chiang Mai, Thailand*

In fast neutron cancer therapy, more than 10% of the cell damage is expected to be caused by recoil nuclei from elastic and inelastic scattering. There are few data for these reactions in the intermediate energy region.

Using the SCANDAL setup at The Svedberg Laboratory in Uppsala, we have measured differential cross sections for elastic scattering on carbon and oxygen at 95 MeV incident neutron energy, covering the angular range $10-85^{\circ}$ (c.m.). We could also obtain differential cross sections for inelastic scattering reactions up to 12 MeV excitation energy. These data are shown to have a significant impact on the determination of recoil kerma coefficients.

*International Workshop on Fast Neutron Detectors and Applications*
*April, 3 - 6, 2006*
*University of Cape Town, South Africa*

[*]Speaker.

[†]Corresponding author, tel. +46 18 471 3788, email address: jan.blomgren@tsl.uu.se

 

PoS(FNDA2006)071

## 1. Introduction

There are a number of new applications under development where neutrons of higher energies than in the traditional applications (nuclear power and nuclear weapons) play a significant role. The most important are transmutation of nuclear waste [1, 2], medical treatment of tumors with fast neutrons [3], and the mitigation of single-event effects in electronics [4]. Cross-section data for neutron-induced nuclear reactions are needed in the intermediate energy region to improve data evaluations and nuclear models which are to be implemented in Monte-Carlo codes in relation to these applications.

Fast neutrons have a potential for efficient cancer therapy treatment. Among the nuclei of interest for this application, we identify the main components of human tissue and bones, which are hydrogen, carbon, oxygen, nitrogen and calcium. The damage inflicted to the cells depends on cross sections for the neutron-induced reactions on these nuclei as well as the energies and masses of the released ionizing particles. A rough evaluation tells us that about 50% of the cell damage is due to neutron-proton ($np$) scattering, about 10% is due to elastic and inelastic scattering on other nuclei, and the rest is due to neutron-induced emission of light ions [3, 5]. Light-ion production at 96 MeV is discussed in separates article by Pomp *et al.* (the MEDLEY facility) and Tippawan *et al.* (data on oxygen) of this workshop [6, 7]. In the present work, we will focus on the $\sim$10% contribution caused by elastic and inelastic neutron scattering on carbon and oxygen.

Recently, our group has measured differential cross sections for neutron scattering on hydrogen, deuterium, carbon and oxygen at The Svedberg Laboratory in Uppsala, using the SCANDAL multi-detector array (details about SCANDAL can be found in Ref. [8] as well as in a paper by Blomgren *et al.* in these proceedings [9]). The primary aim of the experiments was to investigate three-body force effects in elastic neutron-deuteron ($nd$) scattering. The $nd$ data were first published in a short communication [10], and a detailed article has been submitted recently [11]. For normalization purposes, differential cross sections for $np$ scattering and $^{12}$C(n,n) scattering were also measured, using a water and a graphite target, respectively. The measurement on carbon was an extension of the Klug *et al.* data obtained with the same technique [12], and, in addition, elastic and inelastic scattering on oxygen could be extracted. These new carbon and oxygen data were reported together with the $np$ and $nd$ data in Ref. [11]. In this publication, we pointed out that the carbon and oxygen data might be relevant for cancer treatment of tumors with fast neutrons, and we identified angular regions where the accuracy of the theoretical calculations were not satisfying. In the present paper, we will discuss further how the uncertainties in the elastic and inelastic differential cross sections on carbon and oxygen may affect the estimation of the nuclear recoil kerma coefficients at intermediate energies.

## 2. From differential cross sections to kerma coefficients

The partial kerma coefficient $k$ is the average kinetic energy of one type of charged particle produced in matter due to a certain reaction per unit mass divided by the neutron fluence. If the neutrons are propagating inside a living organism, the kerma coefficient is closely related to the probability to cause irreversible DNA damage through the considered reaction. In our case, the reaction is elastic or inelastic scattering at 95 MeV incident neutron energy and the charged

particle is the carbon or oxygen recoil nucleus. Thus, the recoil kerma coefficient is proportional to the integral of the differential cross section multiplied with the solid angle element and the energy of the recoil nucleus:

$$k = N \int E_R \frac{d\sigma}{d\Omega}(\theta) 2\pi \sin\theta d\theta,$$

where $N$ is the inverse nuclear mass of the recoil nucleus, $E_R$ is its kinetic energy in the laboratory system, and $2\pi \sin\theta$ is the solid angle element at the neutron laboratory angle $\theta$.

In Fig. 1, one can follow in a comprehensive way how recoil kerma coefficients are obtained from the differential cross sections. The left panels of the figure correspond to elastic neutron scattering on carbon (here, at 95 MeV), and the right panels correspond to elastic neutron scattering on oxygen. The data are from Mermod *et al.* [11], Klug *et al.* [12], Salmon [13] and Osborne *et al.* [14]. The theoretical curves are predictions from the Koning and Delaroche global potential [15], the Watson global potential [16], Amos *et al.* [17], and Crespo *et al.* [18] (see Refs. [11, 12] for details). In the top panels of the figure, the differential cross sections (in logarithmic scale) are plotted as functions of the neutron scattering angle in the laboratory. The middle panels show the same differential cross sections multiplied with the solid angle element $2\pi \sin\theta$, i.e., they illustrates the angular probability distributions for neutron scattering. As the solid angle vanishes at zero degrees, these distributions are no longer forward-peaked, but rather peak around $10^\circ$. In the bottom panels, the distributions have been weighed with the energy of the recoil nuclei $E_R$, thus illustrating the angular probability distributions for the neutrons to cause cell damage. Back-scattered neutrons transfer more energy to the nuclei than forward-scattered neutrons, and therefore the energy of the recoil nuclei increases with the neutron scattering angle. From these last distributions, which peak at about $16^\circ$, we can deduce that most of the damage is caused by neutrons scattered between 10 and $30^\circ$, but there is still a significant contribution up to $60^\circ$. With this way of plotting, the recoil kerma coefficients are proportional to the area under the distributions.

The data for inelastic scattering on carbon and oxygen at 95 MeV to collective states up to 12 MeV excitation energy (from Ref. [11]) can be treated the same way. The differential cross sections for inelastic scattering multiplied with the solid angle elements and the recoil nuclei energies are plotted in Fig. 2. Here we observe that the main contribution to the kerma from inelastic scattering is between 30 and $60^\circ$, and tends to be underestimated by the calculations.

The values of $k$ for different data sets and different theoretical predictions were evaluated in Refs. [11] and [12], and are reported below in Table 1.

## 3. Concluding comments on the results

Differential cross sections for elastic and inelastic neutron scattering on carbon and oxygen must be well known for a precise evaluation of the damage caused by fast neutrons in human tissue. We have showed that a large angular coverage (up to $60^\circ$) was needed, due to the fact that the recoil nucleus energy increases with increasing scattering angle.

There are large variations in the evaluation of the recoil kerma coefficients $k$ obtained with different models. For elastic scattering, the experimental uncertainty in the nuclear recoil kerma coefficients is about 5%, while it is at least 10% for the theoretical calculations or the values from evaluated data. The ICRU value obtained from evaluated data [19] agrees with the experimental

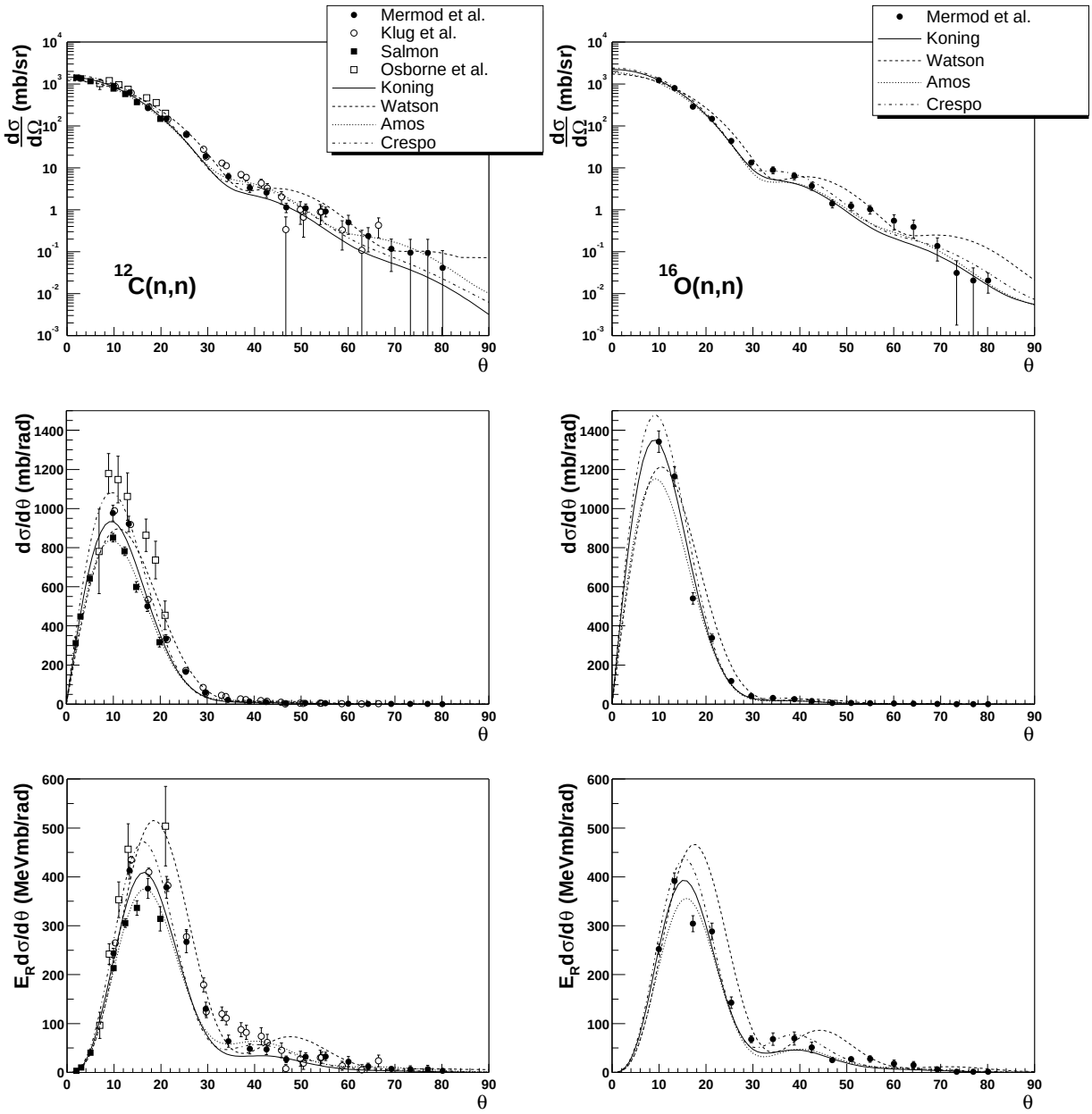


**Figure 1:** Elastic neutron scattering on carbon (left panels) and oxygen (right panels) at 95 MeV. The angle $\theta$ is the neutron scattering angle in the laboratory. The experimental data are from Refs. [11, 12, 13, 14]. Elastic scattering differential cross sections are shown in the top panels; in the middle panels, the differential cross sections were multiplied with the solid angle elements; in the bottom panels, they were further multiplied with the energy of the recoil nuclei. The areas under these last plots are proportional to the nuclear recoil kerma coefficients for elastic scattering.

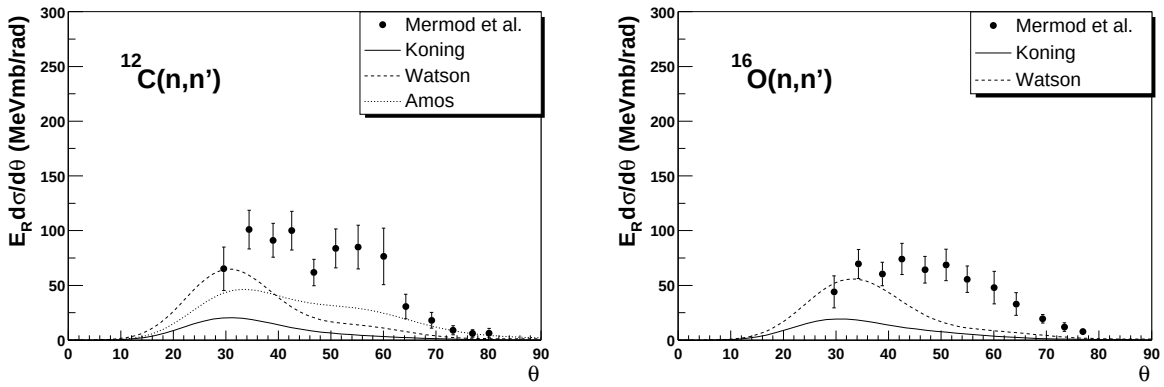


**Figure 2:** Differential cross sections multiplied with the solid angle elements and the energy of the recoil nuclei for inelastic neutron scattering to collective excited states below 12 MeV on carbon (left panels) and oxygen (right panels) at 95 MeV incident neutron energy. The angle $\theta$ is the neutron scattering angle in the laboratory. The experimental data are from Ref. [11]. The areas under these plots are proportional to the nuclear recoil kerma coefficients for inelastic scattering.

| k (fGy·m$^2$) | elastic | inelastic<12 MeV | sum |
|---|---|---|---|
| $^{12}$**C(n,n)** | | | |
| Mermod *et al.* [11] | 0.120±0.007 | 0.047±0.029 | 0.167±0.030 |
| Klug *et al.* [12] | 0.126±0.009 | – | – |
| ICRU [19] | 0.132±0.013 | – | – |
| Koning [15] | 0.102 | 0.007 | 0.109 |
| Watson [16] | 0.145 | 0.023 | 0.168 |
| Amos [17] | 0.105 | 0.026 | 0.131 |
| Crespo [18] | 0.118 | – | – |
| $^{16}$**O(n,n)** | | | |
| Mermod *et al.* [11] | 0.073±0.004 | 0.028±0.006 | 0.101±0.007 |
| ICRU [19] | 0.074±0.007 | – | – |
| Koning [15] | 0.071 | 0.006 | 0.077 |
| Watson [16] | 0.096 | 0.016 | 0.112 |
| Amos [17] | 0.066 | – | – |
| Crespo [18] | 0.082 | – | – |

**Table 1:** Kerma coefficients for the recoil carbon (top) and oxygen (bottom) nuclei from elastic and inelastic neutron scattering at 95 MeV. The inelastic scattering data corresponds to collective excited states with excitation energies below 12 MeV.

values from Refs. [11, 12] within these uncertainties. Among the theoretical models, for elastic scattering on carbon, only Crespo *et al.* seems to give a reasonable prediction, and this is due to the fact that most models are inaccurate in the region $25-35^\circ$. For elastic scattering on oxygen, the prediction closest to the data is provided by the Koning and Delaroche potential. For inelastic scattering on both carbon and oxygen, all models underestimate significantly the data above $40^\circ$. As a consequence, the contribution to the kerma from inelastic scattering lies above the model predictions by about 50%. This underestimation is responsible for an error in the total recoil kerma coefficient (for elastic and inelastic reactions below 12 MeV excitation energy) of about 8%, which is significant.

We wish to thank the technical staff of the The Svedberg Laboratory for enthusiastic and skillful assistance. We are very grateful to Kenneth Amos, Raquel Crespo, Arjan Koning and Antonio Moro for contributions concerning the theoretical part. This work was supported by the Swedish Nuclear Fuel and Waste Management Company, the Swedish Nuclear Power Inspectorate, Ringhals AB, the Swedish Defence Research Agency and the Swedish Research Council.

## References

[1] J. Blomgren, "Experimental Activities at High Energies", Workshop on Nuclear Data for Science & Technology: Accelerator Driven Waste Incineration, Trieste, Italy, Sept. 10-21, 2001, eds. M. Herman, N. Paver and A. Stanculescu, ICTP lecture notes **12**, 327 (2002).

[2] M. Österlund *et al.*, "Elastic neutron scattering studies at 96 MeV for transmutation", these proceedings.

[3] J. Blomgren and N. Olsson, "Beyond Kerma - Neutron Data for Biomedical Applications", Radiat. Prot. Dosim. **103**, 293 (2003).

[4] J. Blomgren, B. Granbom, T. Granlund, and N. Olsson, "Relations Between Basic Nuclear Data and Single-Event Upsets Phenomena", Mat. Res. Soc. Bull. **28**, 121 (2003).

[5] M.B. Chadwick, P.M. DeLuca Jr., and R.C. Haight, "Nuclear data needs for neutron therapy and radiation protection", Radiat. Prot. Dosim. **70**, 1 (1997).

[6] S. Pomp *et al.*, "Light-ion production and fission studies using the MEDLEY facility at TSL", these proceedings.

[7] U. Tippawan *et al.*, "Light charged particle production in 96 MeV neutron induced reactions on oxygen", these proceedings.

[8] J. Klug *et al.*, "SCANDAL−a facility for elastic neutron scattering studies in the 50-130 MeV range", Nucl. Instr. Meth. **A 489**, 282 (2002).

[9] J. Blomgren *et al.*, "SCANDAL−a facility for elastic neutron scattering studies in the 50-130 MeV range", these proceedings.

[10] P. Mermod *et al.*, "Evidence of three-body force effects in neutron-deuteron scattering at 95 MeV", Phys. Rev. C **72**, 061002 (2005).

[11] P. Mermod *et al.*, "95 MeV neutron scattering on hydrogen, deuterium, carbon and oxygen", submitted to Phys. Rev. C (2006).

[12] J. Klug *et al.*, "Elastic neutron scattering at 96 MeV from $^{12}$C and $^{208}$Pb", Phys. Rev. C **68**, 064605 (2003).

[13] G.L. Salmon, "The elastic scattering of 96 MeV neutrons by nuclei", Nucl. Phys. **21**, 15 (1960).

[14] J.H. Osborne *et al.*, "Measurement of neutron elastic scattering cross sections for $^{12}$C, $^{40}$Ca, and $^{208}$Pb at energies from 65 to 225 MeV", Phys. Rev. C **70**, 054613 (2004).

[15] A.J. Koning and J.P. Delaroche, "Local and global nucleon optical models from 1 keV to 200 MeV", Nucl. Phys. **A713**, 231 (2003);
A.J. Koning, S. Hilaire and M.C. Duijvestijn, "TALYS: Comprehensive Nuclear Reaction Modeling", Proceedings of the International Conference on Nuclear Data for Science and Technology, Santa Fe, USA, Sep. 26 - Oct. 1, 2004, CP769, 1154 (2005).

[16] B.A. Watson, P.P. Singh and R.E. Segel, "Optical-Model Analysis of Nucleon Scattering from 1$p$-Shell Nuclei between 10 and 50 MeV", Phys. Rev. **182**, 977 (1969).

[17] K. Amos, P.J. Dortmans, H.V. von Geramb, S. Karataglidis, and J. Raynal, "Nucleon-nucleus scatering: a microscopic nonrelativistic approach", Adv. Nucl. Phys. **25**, 275 (2000); S. Karataglidis, P.J. Dortmans, K. Amos, and R. de Swiniarski, "Multi-$\hbar\omega$ shell model analyses of elastic and inelastic proton scattering from $^{14}$N and $^{16}$O", Phys. Rev. C **53**, 838 (1996).

[18] R. Crespo, R.C. Johnson, and J.A. Tostevin, "Multiple scattering theory of proton elastic scattering at intermediate energies", Phys. Rev. C **46**, 279 (1992).

[19] ICRU Report 63, Nuclear Data for Neutron and Proton Radiotherapy and for Radiation Protection (International Commission on Radiation Units and Measurements, MD, 2000).